CrossMark

ORIGINAL PAPER

# Investigation of electrical properties in La-doped BiFeO$_3$–PbTiO$_3$ thin films prepared by sol–gel method

Dongfang Chen[1] · Shengli Huang[1] · Jianguo Chen[1] · Jinrong Cheng[1]

Abstract La-modified thin films of multiferroic 0.7(Bi$_{1-x}$La$_x$)FeO$_3$–0.3PbTiO$_3$ (BFPT, $x = 0, 0.01, 0.03, 0.05$ and 0.1) solid solution were prepared by sol–gel method. Perovskite BFPT single-phase thin films were successfully synthesized at 600 °C by optimizing several preparation conditions. It was confirmed from X-ray diffraction that BFPT films tend to display sharper peaks with the La concentration, which could be attributed to the changes in grain size and the promotion of La doping in the crystallization. The dielectric constant ε_r also showed a significant increase as compared to those of the undoped BFPT thin films. Furthermore, substitution of small amount of La atoms in BFPT films was effective in reducing leakage current and improving the ferroelectric behavior at a low electric field, which may strongly associated with the grain size and the domain wall density. The P_r and E_c values of 5 mol% La-doped BFPT thin films at room temperature were approximately 23 μC/cm^2 and 80 kV/cm, indicating the potential applications of BFPT thin films in non-volatile ferroelectric memory fields.

Graphical Abstract
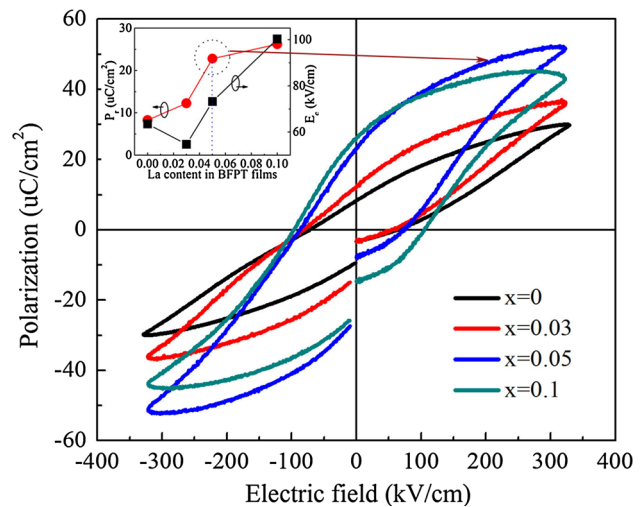
1 Introduction

As a multiferroic material in ambient temperature, BiFeO$_3$ (BFO) is always attracting the attention of researchers for its potential applications in advanced smart devices, such as non-volatile ferroelectric memories and spintronic devices [1, 3]. It is a well-known and representative material, which simultaneously exhibits ferroelectric ($T_C \sim 850$ °C) and antiferromagnetic ($T_N \sim 370$ °C) properties [2–4]. Nevertheless, a series of significant shortcomings of BiFeO$_3$ associated with its electrical performance hampered its potential application [5–8]. Due to the high leakage current and large coercive field of the

✉ Jinrong Cheng
jrcheng@staff.shu.edu.cn

[1] School of Materials Science and Engineering, Shanghai University, Shanghai 200072, People's Republic of China

material, researchers even cannot achieve relatively saturated polarization hysteresis loops at room temperature (RT). To overcome these disadvantages, some methods have been investigated [8, 9]. Qi et al. [8] reported that leakage current density could be greatly reduced by doping several suitable aliovalent ions, but no high polarization characteristics were addressed. Subsequently, it was found that by introducing proper $PbTiO_3$ content, a solid solution of $BiFeO_3$ and $PbTiO_3$ could exhibit optimized ferroelectric and ferromagnetic orderings, even for the desired structural stabilization [9, 10].

$PbTiO_3$ is a stable perovskite ABO_3 compound with a Curie temperature of 490 °C. A solid solution of $BiFeO_3$ and $PbTiO_3$ was reported to exhibit the improved ferroelectric behavior close to the morphotropic phase boundary (MPB) [9]. Unfortunately, due to several drawbacks, like high leakage current, excessive oxygen vacancy density and the volatility of Bi atoms are not remarkably improved [11–13]. Accordingly, A or B site substituted by some elements, which is called site engineering, is a way to fix these drawbacks [11, 14–18]. Sakamoto et al. [18] clarified that B site substitution of Mn-doped $0.7BiFeO_3$–$0.3PbTiO_3$ films could significantly suppress the leakage current density and improve insulating resistance, which agrees well with the other studies [15]. Simultaneously, Lanthanum-doped BFO thin film exhibited overall improvements in ferroelectric and ferromagnetic properties, but some unclear fluctuation still exists [19–22]. Furthermore, previous investigations of La-substituted Bi ion in $BiFeO_3$–$PbTiO_3$ concentrated on the bulk ceramic for its enhanced ferromagnetic property, and reports about La-doped BFPT thin film are rare. In this study, therefore, we mainly demonstrate the effects of La substitution, focusing on the improved dielectric and ferroelectric properties of the thin film by non-aliovalent element doping.

2 Experimental procedures

La-substituted BFPT thin films (up to 10 mol%) were formed by depositing sol–gel solutions on Pt/Si structures. $Bi(NO_3)_3 \cdot 5H_2O$, $Fe(NO_3)_3 \cdot 9H_2O$, $Pb(CH_3COO)_2$, $Ti(OC_3H_7)_4$ and $La(NO_3)_5 \cdot xH_2O$ were used as starting materials and 2-methoxyethanol was used as a solvent for the fabrication of precursor solution. $Pb(CH_3COO)_2$ was 10 mol% excess and $Bi(NO_3)_3 \cdot 5H_2O$ was 2 mol% excess to compensate Pb and Bi loss during heat treatment. The final concentration of BFPT solution was 0.4 mol/L. Then, the stoichiometric solutions of $0.7(Bi_{1-x}La_x)FeO_3$–$0.3PbTiO_3$ were spin-coated at 3500 rpm for 30 s, dried at 200 °C for 3 min, and calcined at 300 °C for 2 min and at 500 °C for 4 min by rapid temperature annealing (RTA). The process of coating and calcination cycle was repeated eight times

until approximately 600-nm-thick films were obtained, which then were annealed at 600 °C for 30 min in the air. Magnetron sputtering was used for depositing Pt top electrodes of 1.256×10^{-3} cm^2 areas through a shadow mask. The crystallographic phases of synthesized BFPT thin films were characterized by X-ray diffraction (XRD) system (Rigaku D/Max-2200V, Japan) using Cu Ka radiation. The surface morphology and microstructure were observed by a field-emission scanning electronic microscope (FESEM, JEOL, JSM-7000F, Japan). Dielectric properties of the samples were measured using an Agilent 4294A impedance analyzer at room temperature. The ferroelectric hysteresis loops and the leakage current density–electric field (J–E) characteristics of the BFPT thin films were characterized by a ferroelectric test system RT6000HVS (Radiant Co.).

3 Results and discussion

Figure 1 shows the XRD patterns of the $0.7(Bi_{1-x}La_x)$-FeO_3–$0.3PbTiO_3$ thin films prepared on Pt/Si substrates after annealing at 600 °C. The films exhibit a single-phase perovskite structure, with no secondary phase addressed. Crystallization is attributed to the stabilization of the perovskite phase by the formation of a solid solution with $PbTiO_3$, because the formation of the second phase, such as the $Bi_2Fe_4O_9$ phase, is due to the low structural stability of perovskite $BiFeO_3$ and the volatility of Bi and Pb ions during the heating process [18]. Meanwhile, the position of the diffraction peaks deviates in the $0.7(Bi_{0.9}La_{0.1})FeO_3$–$0.3PbTiO_3$ film, indicating that the La ion is successfully doped into the perovskite BFPT films and lattice distortion is caused. Furthermore, with increasing La content, the
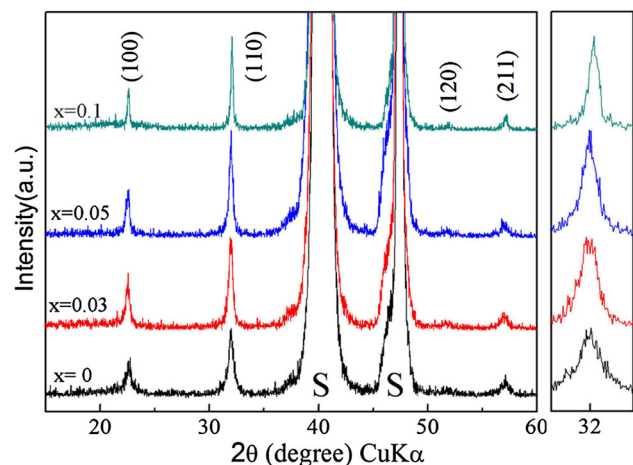

Fig. 1 XRD patterns of $0.7(Bi_{1-x}La_x)FeO_3$–$0.3PbTiO_3$ thin films for $x = 0$, 0.03, 0.05 and 0.1 (Pt-underlayer reflections are marked with S)

relative intensities of (100) and (110) peaks became stronger. Meanwhile, it is observed that the diffraction pattern of the BFPT tends to display a narrower and more intense single peak at $2\theta = 32°$ with the La concentration, which could be attributed to the promotion of La doping in the crystallization. It may also be partly owing to the changes in grain size inside the films. According to Scherrer equation, the larger grain size leads to smaller FWHM, which could be another reason for the sharper peaks.

Figure 2 shows FESEM images of La-doped BiFeO$_3$–PbTiO$_3$ thin films prepared on Pt/Si substrates. The surface morphologies tend to be smoother with increasing La content. Since the SEM images are not suitable to extract the grain size, we use the Scherrer equation ($D = K\gamma/B \cos \theta$, where D is the average thickness of the grains, K is Scherrer constant, B is FWHM, θ is diffraction angle and γ is the wavelength of X-rays) to calculate the grain size of $0.7(Bi_{1-x}La_x)FeO_3–0.3PbTiO_3$ thin films from XRD patterns. The grain size for $x = 0$, 0.03, 0.05 and 0.1 is approximately 39, 50, 55 and 70 nm, respectively. A trend toward larger grain size distribution is found, which indicates that the incorporation of La ions plays a significant role in promoting coalescence of small grains to form large grains. The larger grain size could be the reason for enhanced ferroelectric polarization and reduced leakage current density [11]. Furthermore, the smoother surfaces reflect that more homogeneous domains and reduced domain wall density could be achieved in the La-doped films, which also contributes to the reduced leakage current [3].

Variations in dielectric constant (ε_r) and dielectric dissipation factor (tan δ) as a function of frequency for the La-doped BFPT thin films are shown in Fig. 3, measured in ambient temperature. Dielectric constant of the La-doped thin film exhibits a regular increase with the concentration of La ion, which is found to be approximately 650 at 10^3 Hz of the $0.7Bi_{0.9}La_{0.1}FeO_3–0.3PbTiO_3$ film, indicating the significant effect of La substitution in improving the dielectric constant. However, the dielectric dissipation factor (tan δ) of La-doped samples at the frequencies of 10^3–10^6 Hz fails to exhibit a apparent decline and conversely shows a tendency to increase in high frequency scales when La content reaches 10 mol%. It is obvious that a small amount of La doping has only a small influence on tan δ, which may be due to the bigger grain size of the film and the low charge defects or defect–dipole complexes, such as $V_O^{..}$, V_{Bi}''' or $(V_{Bi}'''\text{-}V_O^{..})'$ [23]. When La content reaches 10 mol%, the increase in tan δ in high frequency scales indicates that the charge carriers in the films fail to follow the external electric field and the maximum electrical energy is transferred to the oscillation ions [24], which may be mainly owing to the relaxation phenomenon inside the films.

Figure 4 shows I–V characteristics of $Pt/Bi_{1-x}La_xFeO_3–PbTiO_3/Pt$ ($x = 0$, 0.03, 0.05 and 0.1) thin film capacitors on Pt/Si structures measured at room temperature. The asymmetric properties of the J–E curves in positive and negative applied field directions are observed in pure BFPT film, which implies that the conduction processes in these films are interface-limited (resistance between the film and
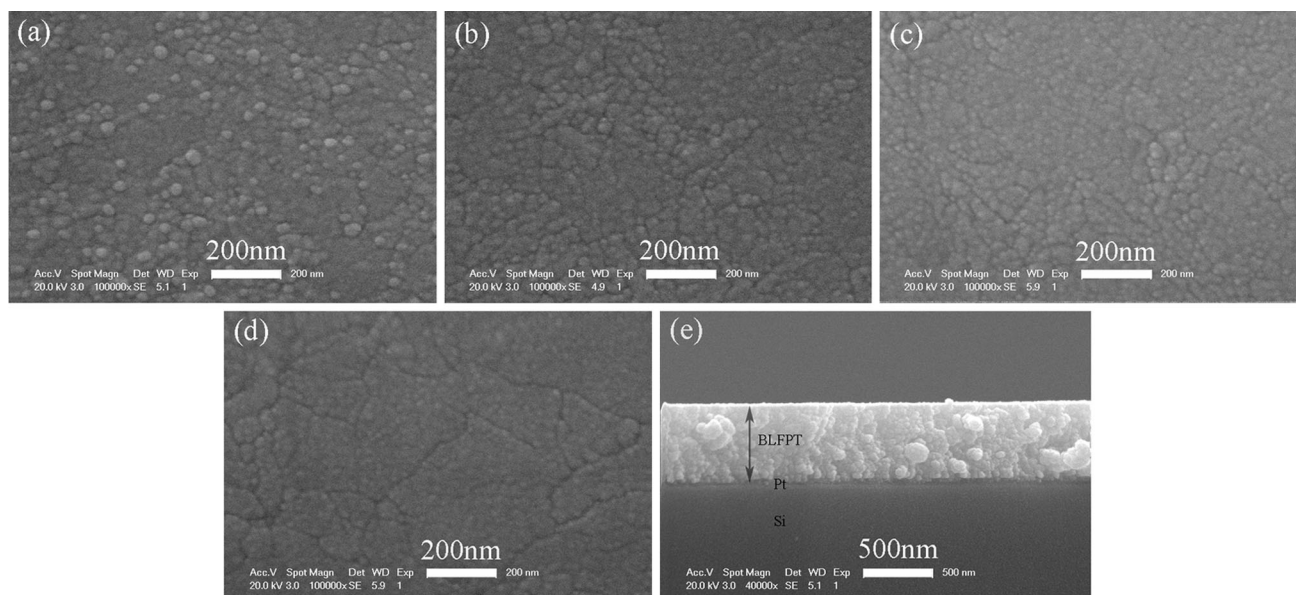

Fig. 2 FESEM images of surface morphologies of $0.7(Bi_{1-x}La_x)FeO_3–0.3PbTiO_3$ thin films for **a** $x = 0$, **b** $x = 0.03$, **c** $x = 0.05$ and **d** $x = 0.1$. **e** A typical FESEM cross-sectional image of the films
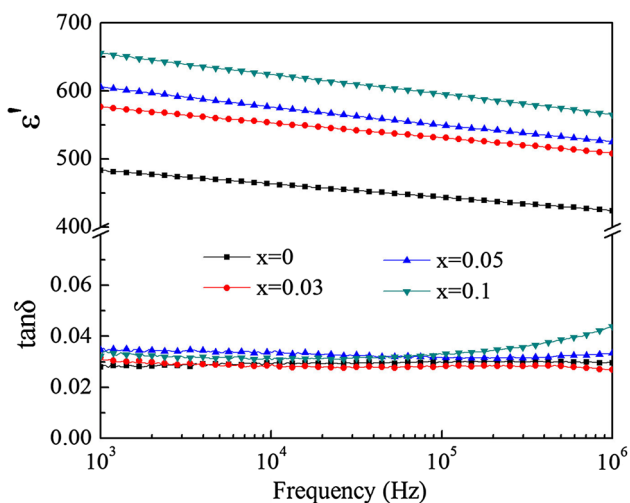
Fig. 3 Dielectric constant K and $\tan\delta$ of $0.7(Bi_{1-x}La_x)FeO_3$–$0.3PbTiO_3$ thin films for $x = 0$, 0.03, 0.05 and 0.1

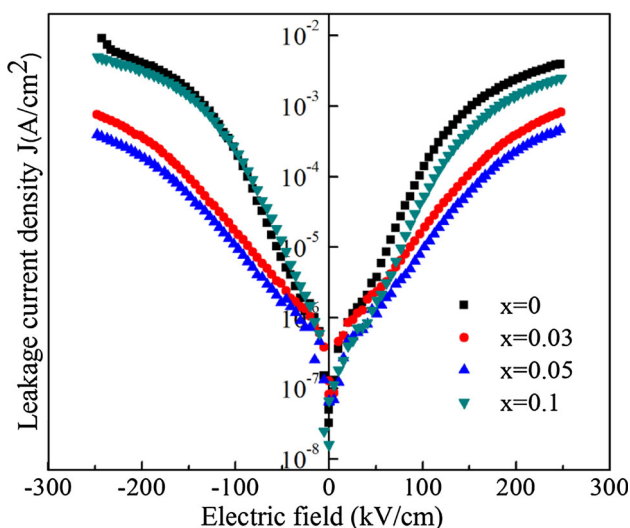**Fig. 4** Leakage current density of $0.7(Bi_{1-x}La_x)FeO_3$–$0.3PbTiO_3$ thin films for $x = 0$, 0.03, 0.05 and 0.1

electrode is much larger than the dielectric thin film). With the La ions doping into the films, the J–E curves become symmetrical, indicating the change in the predominant leakage current conduction from interface-limited to bulk-limited (resistance of the film is larger than interface resistance). This is due to the enhanced insulation of the La-doped films, which determines the leakage current from the interface-limited to bulk-limited conduction. However, when the La content reaches 10 mol%, the conduction process changes back to interface-limited. It is considered that excess La substitution leads to an increase in the electrical conductivity, which could be attributed to the
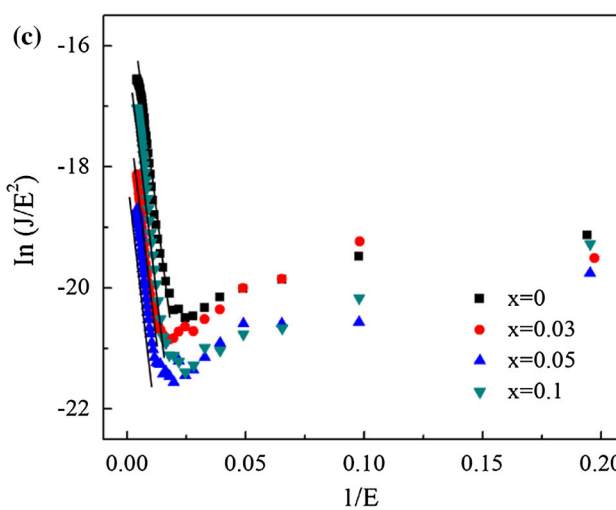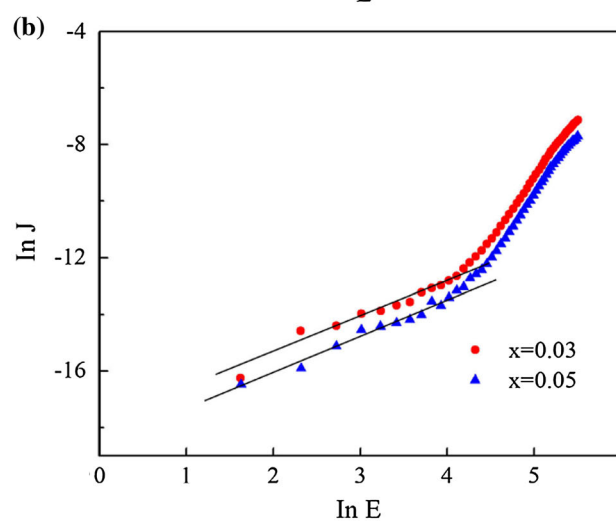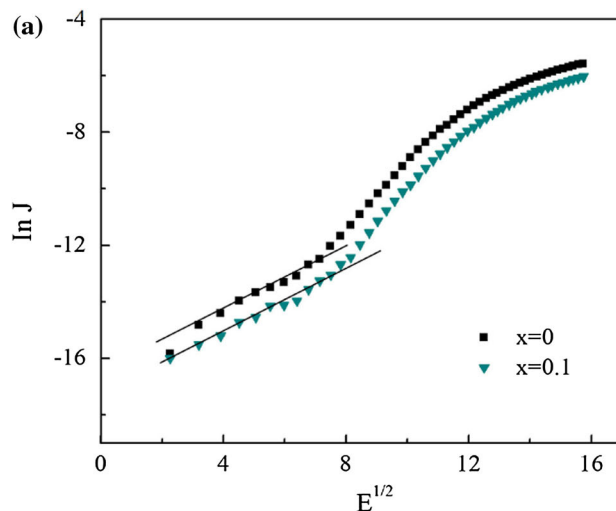

Fig. 5 Leakage currents of $0.7(Bi_{1-x}La_x)FeO_3$–$0.3PbTiO_3$ thin films ($x = 0$, 0.03,0.05 and 0.1) plotted with **a** ln J versus $E^{1/2}$, **b** ln J versus ln E, and **c** ln (J/E^2) versus 1/E
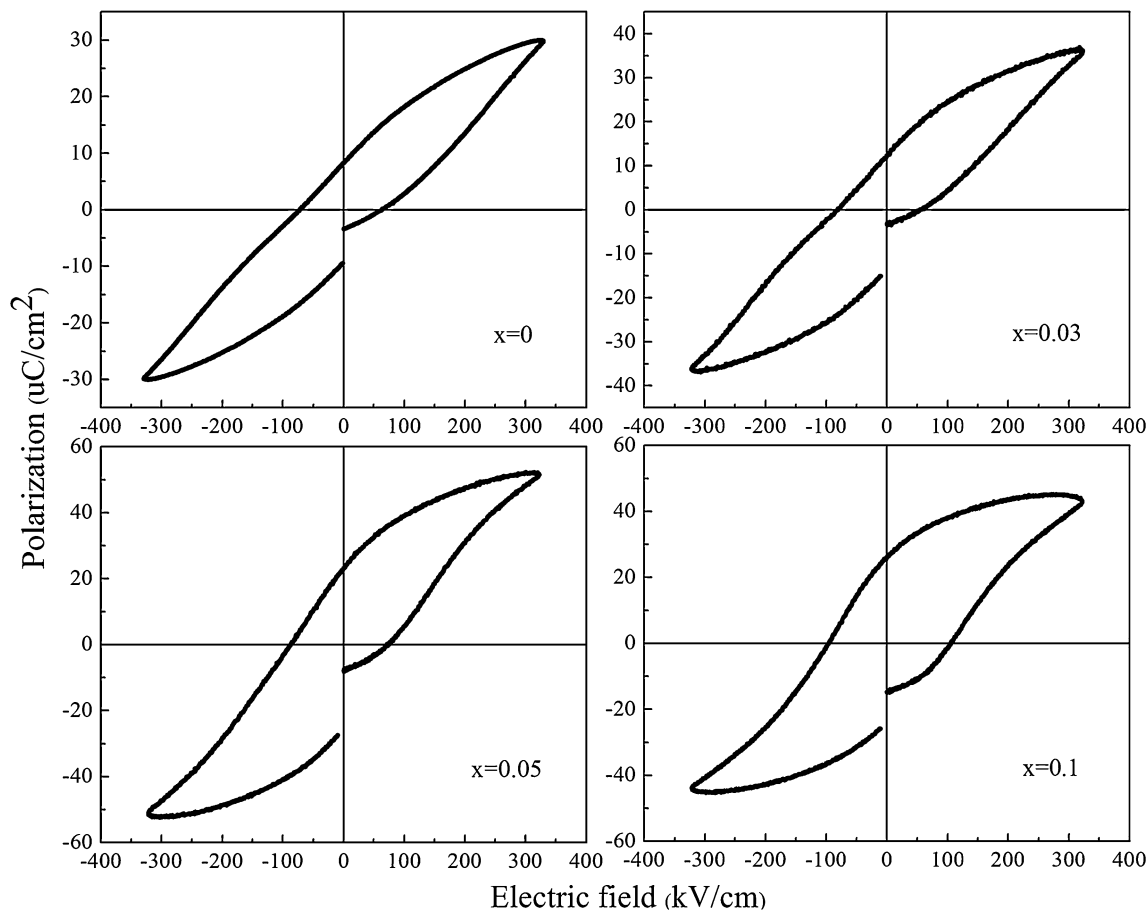
Fig. 6 *P–E* loops of $0.7(Bi_{1-x}La_x)FeO_3$–$0.3PbTiO_3$ thin films for $x = 0$, 0.03, 0.05 and 0.1

stoichiometric imbalance caused by the incorporation of La into the Bi/Pb sites, leading to the formation of Bi-/Pb-rich phases at the grain boundaries (not detectable by XRD analysis) and oxygen vacancies, thus causing extrinsic conduction [17].

According to the data in Fig. 4, the plots for $E^{1/2}$ versus ln J for 0 and 10 mol% La-substituted thin films in the applied field area of Fig. 4 are shown in Fig. 5a. The interface-limited Schottky emission (which can be expressed as $J = AT^2 \exp\left(-\frac{\Phi - \sqrt{q^3 E/\pi \varepsilon_0 \varepsilon}}{kT}\right)$ [25], where A is a constant, T is absolute temperature, E is the electric field, k is Boltzmann's constant, Φ is the barrier height, ε_0 is the permittivity of free space and ε is the optical dielectric permittivity of thin film) is considered to be the dominant conduction mechanism in a relatively low applied field area through a straight fit in Fig. 5a. Meanwhile, the plots for ln E versus ln J of the films with 3 and 5 mol% La doping are also displayed in Fig. 5b. The linear fitting with a slope of approximately 0.5 in Fig. 5b suggests that the predominant electric conduction in the low electric field range is the Ohmic conduction (the Ohmic conduction mechanism

is evident from the linear conduction characteristic of $J \propto E$), which results from the reduction of domain walls and the oxygen vacancies in the La-doped BFPT films. The presence of La dopant is effective in controlling the volatility of Bi atoms and thereby suppresses the oxygen vacancy concentration because the energy of the La–O bond (789.6 ± 8 kJ/mol) is much stronger than that of the Bi–O bond (337.2 ± 12 kJ/mol) [19]. Simultaneously, La substitution in Bi site may also contribute to stabilizing the valance state of Fe ions, which would suppress the hopping of electrons from Fe^{2+} to Fe^{3+} and as a result reduce the concentration of oxygen vacancy in the BFPT films [26]. Since the BFO-based thin films tend to exhibit relatively low insulating resistance which is caused by defects and non-stoichiometric compositions in the materials, the reduced leakage current density would contribute to the promotion of the performance. In this case, the obtained thin films of La substitution display better insulating properties as compared to the undoped BFPT films. However, the linear fitting in Fig. 5c reveals that the predominant electric conduction in all components of the films is the Fowler–Nordheim (FN) tunneling process (which can
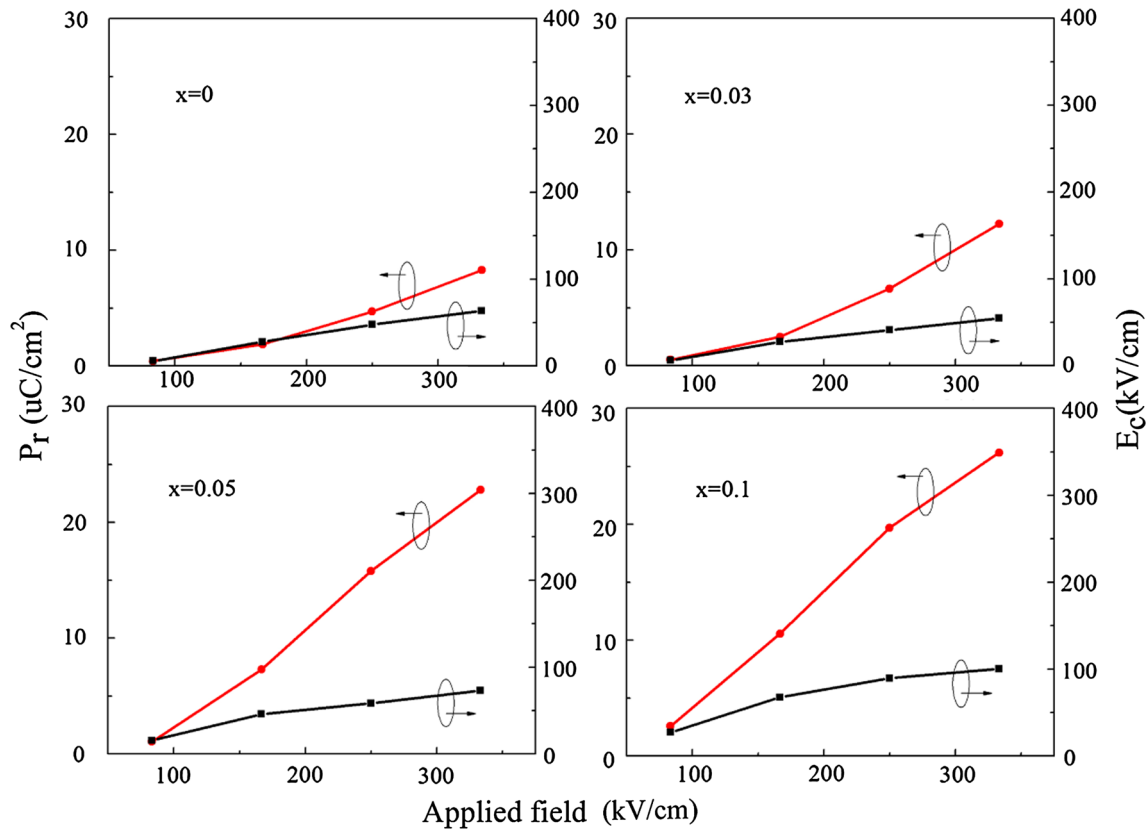
Fig. 7 Electric field dependence of remnant polarization (P_r) and coercive field (E_c) of $0.7(Bi_{1-x}La_x)FeO_3–0.3PbTiO_3$ thin films for $x = 0$, 0.03,0.05 and 0.1

be expressed as $J = AE^2 \exp\left(-\frac{B\Phi_i^{-3/2}}{E}\right)$ [25], where A and B are constants, E is the applied electric field and Φ_i is potential barrier height) in a relatively high applied field area. The charge carriers were tunneling through the barrier into the conduction band of the films from Pt electrodes, which led to a rapid increase in leakage current.

The polarization versus electric field ($P–E$) hysteresis loops of BFPT films measured at room temperature are shown in Fig. 6. It is found that the hysteresis loop for a pure BFPT film was much more flat when it was measured with a frequency of 2×10^3 Hz. Simultaneously, La-doped films display the difference in the shape of hysteresis loops. $P–E$ hysteresis loops of the films tend to exhibit a well-defined saturation and asymmetry with the increase in La substitution, and the 5 mol% La-substituted film exhibits the best ferroelectric behavior with the remnant polarization (P_r) of 23 $\mu C/cm^2$ and coercive field (E_c) of 80 kV/cm. It is obvious that the La dopant can significantly enhance the ferroelectricity in low electric field. Figure 7 shows the electric field dependence of remnant polarization and coercive field in the La-substituted films. As shown in the figure, with increasing La content, it is easier to get a relatively high remnant polarization at a low electric field.

In other words, when pure BFPT films still need a higher applied electric field to achieve saturated $P–E$ hysteresis loops, it has already tend to demonstrate the relatively saturated hysteresis loops in 5–10 mol% La doped BFPT films. The smoother surface and larger grain size play a positive role in promoting the inversion of the domain inside the films, which is reflected in the FESEM images. According to Yan et al.'s report, the domain structures of the La-doped films show more homogeneous domains and reduced domain wall density [23]. Homogeneous domains and bigger grain sizes contribute to the reversion of domain and reduced domain wall density, leading to a better insulation since certain domain walls in the film are much more conductive than the domains themselves [3], which in turn leads to the enhanced ferroelectric properties.

4 Conclusions

Ferroelectric $0.7(Bi_{1-x}La_x)FeO_3–0.3PbTiO_3$ ($x = 0$, 0.01, 0.03, 0.05 and 0.1) thin films with a thickness of 600 nm were synthesized by sol–gel method. La doping proved that it could promote the crystallization and grain growth of the films. The dielectric constant (ε_r) could also be improved

through substitution of La ions, while the dielectric dissipation factor (tan δ) of La-doped samples at the frequencies of 10^3–10^6 Hz exhibited no significant changes. Among the BFPT thin films with various La ion concentrations, 5 mol% La substitution of the film demonstrated improved insulation and optimized ferroelectric behavior with remnant polarization (P_r) of 23 $\mu C/cm^2$ and coercive field (E_c) of 80 kV/cm, which benefited from the bigger grain size and reduced domain wall density. By controlling the volatility of Bi atoms and stabilizing the valence of Fe ions, La dopant effectively decreased the concentration of oxygen vacancy and therefore enhanced the insulating properties of the films. All of these make this material a promising candidate in low electric field for practical application.

References

1. Martin LW, Ramesh R (2012) Acta Mater 60:2449
2. Wang J, Neaton JB, Zheng H, Nagarajan V, Ogale SB, Liu B, Viehland D, Vaithyanathan V, Schlom DG, Waghmare UV, Spaldin NA, Rabe KM, Wuttig M, Ramesh R (2003) Science 299:1719
3. Catalan G, Scott JF (2009) Adv Mater 21:2463
4. Ryu S, Son JY, Shin Y-H, Jang HM, Scott JF (2009) Appl Phys Lett 95:242902
5. Cheng ZX, Wang XL, Kimura H, Ozawa K, Dou SX (2008) Appl Phys Lett 92:092902
6. Lee D, Kim MG, Ryu S, Jang HM, Lee SG (2005) Appl Phys Lett 86:222903
7. Lee YH, Wu JM, Lai CH (2006) Appl Phys Lett 88:042903
8. Qi X, Dho J, Tomov R, Blamire MG, MacManus-Driscoll JL (2005) Appl Phys Lett 86:062903
9. Khan MA, Comyn TP, Bell AJ (2007) Appl Phys Lett 91:032901
10. Gupta S, Garg A, Agrawal DC, Bhattacharjee S, Pandey D (2009) J Appl Phys 105:014101
11. Das SR, Bhattacharya P, Choudhary RNP, Katiyar RS (2006) J Appl Phys 99:066107
12. Wang SY, Xue Qiu J, Gao Yu, Feng W, Zheng JX, Yu DS, Li DJ (2011) Appl Phys Lett 98:152902
13. Benfang Yu, Li M, Liu J, Guo D, Pei L, Zhao X (2008) J Phys D Appl Phys 41:065003
14. Singh SK, Ishiwara H, Sato K, Maruyama K (2007) J Appl Phys 102:094109
15. Zhu W-M, Ye Z-G (2006) Appl Phys Lett 89:232904
16. Mishra KK, Satya AT, Bharathi A, Sivasubramanian V, Murthy VRK, Arora AK (2011) J Appl Phys 110:123529
17. Cótica LF, Estrada FR, Freitas VF, Dias GS, Santos IA, Eiras JA, Garcia D (2012) J Appl Phys 111:114105
18. Sakamoto W, Iwata A, Yogo T (2008) J Appl Phys 104:104106
19. Kim W-H, Son JY (2013) Appl Phys Lett 103:132907
20. Freitas VF, Protzek OA, Montoro LA, Gonçalves AM, Garcia D, Eiras JA, Guo R, Bhalla AS, Otica LFC, Santos IA (2014) J Mater Chem C 2:364372
21. Gao F, Cai C, Wang Y, Dong S, Qiu XY, Yuan GL, Liu ZG, Liu JM (2006) J Appl Phys 99:094105
22. Singh SK, Maruyama K, Ishiwara H (2007) J Phys D Appl Phys 40:2705
23. Yan F, Zhu TJ, Lai MO, Lu L (2010) Scr. Mater. 63:780
24. Zheng RY, Wang J, Ramakrishna S (2008) J Appl Phys 104:034106
25. Jianlong X, Jia Z, Zhang N, Ren T (2012) J Appl Phys 111:074101
26. Singh SK, Ishiwara H (2006) J Appl Phys 100:064102